

# COMPUTATION OF QUASI-PERIODIC INVARIANT TORI IN THE RESTRICTED THREE-BODY PROBLEM

Zubin P. Olikara\* and Kathleen C. Howell†

Quasi-periodic orbits lying on invariant tori in the circular restricted three-body problem offer a broad range of mission design possibilities, but their computation is more complex than that of periodic orbits. A preliminary framework for directly computing these invariant tori is presented including a natural parameterization and a continuation scheme. The numerical methodology is demonstrated by generating families of quasi-periodic tori with fixed Jacobi constant values that emanate from periodic orbits about the Earth-Moon libration points.

## INTRODUCTION

Invariant manifold theory provides a powerful tool for understanding dynamical behavior in the circular restricted three-body problem (CR3BP). In particular, invariant tori and their associated stable, unstable, and center manifolds serve as a foundation for the system dynamics. The equilibrium, or libration, points (zero-dimensional tori) as well as periodic orbits (one-dimensional tori) in the CR3BP have been extensively studied for their applications to mission design.<sup>1,2</sup> Quasi-periodic orbits lying on higher-dimensional tori also offer a broad range of mission possibilities, but additional complexities are involved in their computation. The goal of the current work is the preliminary development of a framework for computing quasi-periodic invariant tori in the CR3BP.

From the investigation of quasi-periodic orbits, along with lower-dimensional invariant objects, an expanded design space and a more structured view of the dynamical environment becomes available.<sup>3</sup> Of particular interest are two-dimensional invariant tori, which include quasi-periodic orbits such as Lissajous trajectories and quasi-halos. Because of the special character of the CR3BP, an entire family of these tori is present at a fixed energy level. These quasi-periodic orbits often share many of the advantages, such as accessibility and line-of-sight, that are characteristic of the underlying periodic orbit. Many quasi-periodic orbits also possess their own stable and unstable manifolds and, thus, may actually offer more efficient transfer options, especially in a higher-fidelity model, than an underlying periodic orbit. In addition, quasi-periodic structures supply options for formation flying and the design of satellite constellations.

---

\*Graduate Student, School of Aeronautics and Astronautics, Purdue University, West Lafayette, Indiana 47907; Student Member AIAA.

†Hsu Lo Professor of Aeronautical and Astronautical Engineering, School of Aeronautics and Astronautics, Purdue University, West Lafayette, Indiana 47907; Fellow AAS; Associate Fellow AIAA.

From a dynamical systems perspective, the computation of invariant tori is an important capability and various strategies have been developed. However, only some of these computational approaches have been applied to problems in astrodynamics. For Hamiltonian systems such as the CR3BP, semi-analytic methods are available for computing invariant tori. Two such methods are center manifold reduction<sup>4</sup> and the Poincaré-Lindstedt method.<sup>5</sup> These local methods offer a thorough view of the dynamics in the vicinity of the libration points, but both are limited by their regions of convergence. Specialized algebraic manipulators are often required as well, which can create difficulties in the implementation. Purely numerical methods offer an alternate approach to overcome these limitations. Such numerical algorithms typically focus on either the invariant curves of a map or the invariant tori of the flow in a vector field. For example, Jorba and Olmedo<sup>6,7</sup> use a Fourier series to describe an invariant curve representing the intersection of an invariant torus with a Poincaré section in a perturbed CR3BP. Gómez and Mondelo<sup>8</sup> develop the Fourier expansion associated with a curve lying on the surface of a two-dimensional torus in the CR3BP, and use an invariance condition based on multiple shooting.

The focus of this current analysis is also the direct computation of two-dimensional invariant tori, but the approach here can be generalized to higher-dimensional tori without much difficulty. To avoid the dependence on a surface of section, the development of a computational scheme is based on a method developed by Schilder, Osinga, and Vogt.<sup>9</sup> This approach is designed for generic dynamical systems, but can be applied to trajectory design with some modifications relevant to systems with special structure such as the CR3BP. In particular, for a generic dynamical system to possess a family of two-dimensional tori, at least one system parameter is required. For a Hamiltonian system, this family can exist without any external parameters. A scheme is developed where additional, “artificial” parameters are incorporated in the CR3BP such that a generic method can be applied but the dynamics are unaffected.

In contrast to the work of Gómez and Mondelo, computation of tori in the analysis here incorporates an invariance partial differential equation (PDE). This strategy enforces the CR3BP vector field on the quasi-periodic torus to be everywhere tangent. Central differencing of this PDE yields a system of equations that is straightforward to solve using a Newton method along with a sparse linear system solver. Although this process results in a less precise approximation of the invariant torus, no forward integration is necessary, as opposed to a method based on multiple shooting. Both computational approaches produce a natural, global parameterization of the torus (i.e., any state on the torus can be identified by two angles,  $\theta_1, \theta_2$ ), but a more efficient evaluation of the corresponding state is available with the invariance PDE method. The availability of a multiple-parameter spline approximation allows quasi-periodic trajectories on the surface of the invariant torus to quickly be determined from various starting points. If greater accuracy is required, an approximate quasi-periodic trajectory is a suitable input to a corrections process. Once a design is completed in the CR3BP, the trajectory can be transitioned to a higher-fidelity model.

An additional benefit of the current invariance PDE approach is that continuation proceeds in an intuitive manner without the introduction of constraints on the components of a Fourier expansion. Since two-dimensional quasi-periodic tori in the CR3BP exist in two-parameter families, there are a variety of options for their continuation. The family can first be reduced to a single parameter by fixing the ratio of basic frequencies,  $\omega_2/\omega_1$  (where

$\omega_1 = \dot{\theta}_1, \omega_2 = \dot{\theta}_2$ ), or the Jacobi constant,  $C$ , in the CR3BP. The latter option is selected for the current study and is particularly applicable for mission design where the goal is often a set of orbits that exist at a certain energy level. Pseudo-arclength continuation is then used to generate constant energy families of quasi-periodic tori, such as a family of Lissajous trajectories in the Earth-Moon system originating from a planar Lyapunov periodic orbit and terminating with a vertical periodic orbit at the corresponding energy level.

## CIRCULAR RESTRICTED THREE-BODY PROBLEM

In the CR3BP, the gravitational interaction of three bodies, one with infinitesimal mass, is modeled. The two massive bodies rotate about their barycenter in circular orbits. Consider a frame that rotates along with these primary bodies such that unit vector  $\mathbf{e}_1$  is directed from the larger body to the smaller body. Unit vector  $\mathbf{e}_3$  is parallel to the system's angular momentum vector, and  $\mathbf{e}_2$  lies in the plane of the primaries completing the right-handed system. Nondimensionalization yields a mass parameter  $\mu \in [0, 1/2]$ . Given the scalar, potential-like function,

$$U(\mathbf{q}) = \frac{1-\mu}{\|\mathbf{q} + \mu\mathbf{e}_1\|} + \frac{\mu}{\|\mathbf{q} + (\mu-1)\mathbf{e}_1\|} + \frac{1}{2}(x^2 + y^2), \quad (1)$$

the CR3BP system dynamics can be represented by the vector equation of motion,

$$\begin{pmatrix} \dot{\mathbf{q}} \\ \dot{\mathbf{v}} \end{pmatrix} = \dot{\mathbf{x}} = \mathbf{f}(\mathbf{x}) = \begin{pmatrix} \mathbf{v} \\ \partial U(\mathbf{q})/\partial \mathbf{q} + 2\mathbf{v} \times \mathbf{e}_3 \end{pmatrix}, \quad (2)$$

where the  $\mathbf{q} = (x, y, z) \in \mathbb{R}^3$  is the rotating-frame position of the third body with respect to the system barycenter, and  $\mathbf{v} = (v_x, v_y, v_z) \in \mathbb{R}^3$  is its corresponding relative velocity. Like all dependent variables,  $\mathbf{q}$  and  $\mathbf{v}$  are defined as column vectors. The complete state is denoted by vector  $\mathbf{x} = (\mathbf{q}, \mathbf{v}) \in \mathbb{R}^6$ .

The first-order ordinary differential equation (2) admits an integral of motion,

$$C(\mathbf{x}) = 2U(\mathbf{q}) - \|\mathbf{v}\|^2, \quad (3)$$

which is often denoted the Jacobi constant. If the dynamics are derived from a Hamiltonian viewpoint, the Hamiltonian  $H = -C/2$  is an energy-like function. Thus, the value  $C(\mathbf{x})$  in equation (3) decreases when the state  $\mathbf{x}$  is increased to a higher energy level.

There are five well-known libration points, which are equilibrium solutions to equation (2). A linearization relative to these constant solutions reveals a center component corresponding to periodic orbits that emanate from the libration points. One family of planar Lyapunov orbits emerge from each of the collinear libration points,  $L_1$ ,  $L_2$ , and  $L_3$ , and planar short- and long-period families emerge from the triangular points,  $L_4$  and  $L_5$ , as well. In addition, vertical families of periodic orbits exist in the vicinity of all the libration points.<sup>10</sup> Many of these periodic orbits also possess a center component corresponding to quasi-periodic motion about the orbit.<sup>3</sup>

## QUASI-PERIODIC INVARIANT TORI

Since quasi-periodic motions appear in various dynamical systems, it is possible to consider their appearance in generic systems without first assuming any special structure. The

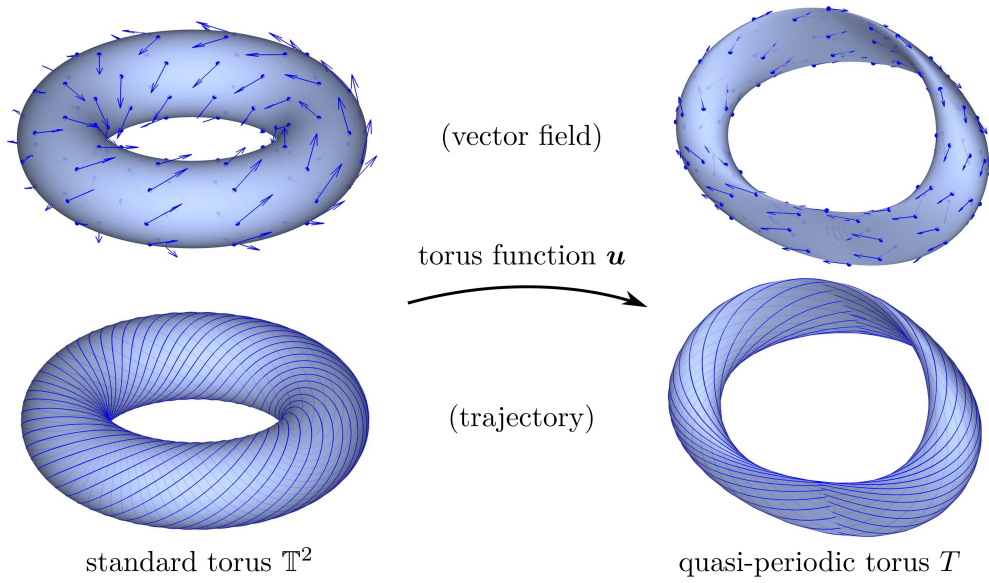


**Figure 1. Diffeomorphism from standard torus to quasi-periodic torus.**

equation of motion (2) in the CR3BP can be considered generically as an autonomous ordinary differential equation of the form

$$\dot{\mathbf{x}} = \mathbf{f}(\mathbf{x}, \boldsymbol{\lambda}), \quad (4)$$

where  $\mathbf{x} \in \mathbb{R}^n$  is a state vector, and  $\mathbf{f}$  defines a differentiable vector field depending on external parameters  $\boldsymbol{\lambda} \in \mathbb{R}^m$ . The notation is generally selected to be consistent with Schilder et al.<sup>9</sup> If it is not necessary to express the parameters  $\boldsymbol{\lambda}$  explicitly, equation (4) can be written simply as  $\dot{\mathbf{x}} = \mathbf{f}(\mathbf{x})$ . Assuming that the equation possesses a quasi-periodic orbit as a solution, this orbit densely covers the surface of a torus. In other words, if  $\phi_t$  is the flow generated by the vector field  $\mathbf{f}$ , then the closure of the quasi-periodic orbit is an invariant torus  $T := \text{cl} \{ \phi_t(\mathbf{x}_0) \mid t \in \mathbb{R} \}$ , where  $\mathbf{x}_0$  is the starting point of the trajectory.

It is often preferable, especially from a computational standpoint, to view the torus directly as an invariant object, independent of a particular trajectory on its surface. Consider a standard  $p$ -dimensional torus  $\mathbb{T}^p := (\mathbb{S}^1)^p = (\mathbb{R}/2\pi\mathbb{Z})^p$  parameterized by angles  $\boldsymbol{\theta} \in [0, 2\pi)^p$ . A vector field  $\mathbf{g}$  on this torus is defined as inducing *quasi-periodic flow* if over the entire surface,

$$\dot{\boldsymbol{\theta}} = \mathbf{g}(\boldsymbol{\theta}) = \boldsymbol{\omega}, \quad (5)$$

where  $\boldsymbol{\omega} = (\omega_1, \dots, \omega_p) \in \mathbb{R}^p$  is a constant vector comprised of the flow's internal frequencies, none of which are resonant with each other. If there exists a diffeomorphism\*  $\mathbf{u} : \mathbb{T}^p \rightarrow T \subset \mathbb{R}^n$  such that torus  $T := \{ \mathbf{u}(\boldsymbol{\theta}) \mid \boldsymbol{\theta} \in \mathbb{T}^p \}$  is invariant (i.e., the vector field induces dynamics that are restricted to the torus) and  $\mathbf{u}^{-1}$  transforms  $\mathbf{f}|_T$  to a constant vector field  $\dot{\boldsymbol{\theta}} = \boldsymbol{\omega}$ , then  $T$  is a *quasi-periodic torus*. An illustration of the torus function  $\mathbf{u}$  for a  $p = 2$ -dimensional torus appears in Figure 1. Note that for  $n > 3$ , a projection of  $T$  onto three-dimensional space can intersect itself, as seen in the figure, but this self-intersection is only of the projection and not the torus itself.

---

\*A *diffeomorphism* is a map between manifolds such that the map and its inverse are differentiable.

## Invariance PDE

The condition on torus function  $\mathbf{u}$  such that  $T$  is invariant, specifically a  $p$ -dimensional quasi-periodic torus, can be represented by a partial differential equation. For motion on the torus, the state  $\mathbf{x}$  in equation (4) can be replaced by the function  $\mathbf{u}$ . Applying the chain rule to the left-hand side of this equation, the following relationship is obtained,

$$\dot{\mathbf{u}} = \sum_{i=1}^p \frac{\partial \mathbf{u}}{\partial \theta_i} \frac{d\theta_i}{dt} = \mathbf{f}(\mathbf{u}). \quad (6)$$

Including equation (5) for quasi-periodic flow in the above relation, yields the invariance PDE,

$$\sum_{i=1}^p \omega_i \frac{\partial \mathbf{u}}{\partial \theta_i} = \mathbf{f}(\mathbf{u}). \quad (7)$$

This equation guarantees that at any point  $\boldsymbol{\theta}$  on the torus, the vector field  $\mathbf{f}$  is a linear combination of the vectors  $\{\partial \mathbf{u} / \partial \theta_1, \dots, \partial \mathbf{u} / \partial \theta_p\}$ , which form a basis for the tangent space of the torus. A solution  $(\mathbf{u}, \boldsymbol{\omega})$  to this PDE produces a quasi-periodic invariant torus  $T$  with a natural parameterization by angles  $\boldsymbol{\theta}$ . Also note that for the case of an equilibrium point ( $p = 0$ ) or a periodic orbit ( $p = 1$ ), equation (7) becomes the familiar invariance relations. The current analysis will primarily consider the two-dimensional quasi-periodic torus case ( $p = 2$ ).

## Phase Condition

Given that the quasi-periodic torus  $T$  is defined in terms of the angles  $\boldsymbol{\theta}$ , the associated phase of each remains to be constrained. If the torus function  $\mathbf{u}$  satisfies equation (7), then it is possible to define another solution  $\mathbf{u}_s$ , where  $\mathbf{u}_s(\boldsymbol{\theta}) := \mathbf{u}(\boldsymbol{\theta} + \mathbf{s})$  with phase shift  $\mathbf{s} \in \mathbb{T}^p$ , that corresponds to the *same* torus  $T$ . Given a solution  $\mathbf{u}_0$  corresponding to a *nearby* torus  $T_0$  in the family, it is common to select the phase of  $\mathbf{u}$  such that  $\|\mathbf{u} - \mathbf{u}_0\|^2 = \langle \mathbf{u} - \mathbf{u}_0, \mathbf{u} - \mathbf{u}_0 \rangle$  is an extremum, particularly a minimum. The inner product between two torus functions  $\mathbf{v}, \mathbf{w}$  is defined to be

$$\langle \mathbf{v}, \mathbf{w} \rangle := \frac{1}{(2\pi)^p} \int_{\mathbb{T}^p} \langle \mathbf{v}(\boldsymbol{\theta}), \mathbf{w}(\boldsymbol{\theta}) \rangle d\boldsymbol{\theta}. \quad (8)$$

Schilder et al.<sup>9</sup> introduce the phase condition

$$\left\langle \frac{\partial \mathbf{u}_0}{\partial \theta_i}, \mathbf{u} \right\rangle = 0, \quad i = 1, \dots, p, \quad (9)$$

which guarantees that  $\|\mathbf{u} - \mathbf{u}_0\|^2$  is an extremum. This condition fixes the  $p$  free phases for the torus  $T$  and generalizes the integral phase condition that is often used for periodic orbits.

## Families of Tori

The existence of solutions  $(\mathbf{u}, \boldsymbol{\omega})$  to equations (7) and (9) is based on Kolmogorov-Arnold-Moser (KAM) theory. The details are not considered in the current analysis, but some of the major results are significant for this development. For a generic system (one

without structure, i.e., dissipative), an invariant  $p$ -dimensional torus typically lies in an  $m$ -parameter family, where  $m$  is the number of external parameters ( $\boldsymbol{\lambda} \in \mathbb{R}^m$ ). On the other hand, for a Hamiltonian system an invariant  $p$ -torus (for  $p \leq n/2$ ) typically lies in a  $(p+m)$ -parameter family.<sup>11</sup> This means it requires  $p+m$  variables to identify a particular member of the family, even though there are only  $m$  external parameters.

Assuming there exists a  $q$ -parameter family of  $p$ -tori, a Hamiltonian system will, therefore, have  $p$  fewer *external* parameters than a generic system. These “missing” parameters must be incorporated to apply a method designed for computing quasi-periodic tori of generic systems. The CR3BP, which is a Hamiltonian system with  $m = 0$  external parameters (assuming mass parameter  $\mu$  is fixed), has two-parameter families of two-dimensional tori. Thus, two “artificial” external parameters must be incorporated to treat this system as generic.

Due to the behavior near resonances, the actual families of tori belong to a Cantor set. However, the computational approach presented here can step over resonances along a family that are sufficiently weak and is independent of the stability of the tori.<sup>9</sup> In addition, the frequency vector  $\boldsymbol{\omega}$  corresponding to a torus  $T$  is unique up to a transformation of the form  $\boldsymbol{\omega} \mapsto \mathbf{A}\boldsymbol{\omega}$ , where  $\mathbf{A}$  is a unimodular matrix.<sup>†</sup> The transformed frequency is associated with a different parameterization  $\mathbf{u}$  of the torus  $T$ , but all of the parameterizations correspond to an identical quasi-periodic flow on the torus.<sup>8,11</sup> This property will be useful when initializing the frequencies associated with a torus emanating from a periodic orbit.

## NUMERICAL IMPLEMENTATION

### Initialization from Periodic Orbit

It is possible to develop a linear approximation of a quasi-periodic torus relative to a periodic orbit with a center component. A periodic orbit with period  $T_1$  can be viewed as a one-dimensional ( $p = 1$ ) invariant torus. Let  $\bar{\mathbf{u}} : \mathbb{T}^1 \rightarrow \mathbb{R}^n$  be its torus function, and  $\omega_1 = 2\pi/T_1$  be the associated frequency. If  $\phi_t$  is the flow generated by the vector field from equation (4), the state transition matrix  $D\phi_t : \mathbb{R}^n \rightarrow \mathbb{R}^n$  represents the linearized dynamics and is defined as

$$D\phi_t(\mathbf{x}_0) := \frac{\partial \phi_t}{\partial \mathbf{x}_0}(\mathbf{x}_0). \quad (10)$$

A related matrix  $\Phi_{\Delta\theta_1}(\theta_1)$  can be defined specifically for a periodic orbit  $\bar{\mathbf{u}}$ , corresponding to its state transition matrix from initial point  $\bar{\mathbf{u}}(\theta_1)$  to any downstream point  $\bar{\mathbf{u}}(\theta_1 + \Delta\theta_1)$ ,

$$\Phi_{\Delta\theta_1}(\theta_1) := D\phi_t(\bar{\mathbf{u}}(\theta_1))|_{t=\Delta\theta_1/\omega_1}. \quad (11)$$

The state transition matrix over one period,  $\Phi_{2\pi}(\theta_1)$ , is labeled the monodromy matrix.

Consider a periodic orbit with a center component. This corresponds to a monodromy matrix  $\Phi_{2\pi}(0)$  that possesses an eigenvalue  $e^{i\alpha} = \cos \alpha + i \sin \alpha$  on the unit circle and an associated complex eigenvector  $\mathbf{y}(0) \in \mathbb{C}^n$ ,  $\|\mathbf{y}(0)\| = 1$ . It can be demonstrated that the monodromy matrix  $\Phi_{2\pi}(\theta_1)$  also has the same eigenvalue  $e^{i\alpha}$  and an eigenvector  $\Phi_{\theta_1}(0)\mathbf{y}(0)$ . Since any eigenvector times a complex scalar is also an eigenvector, the desired form of the

<sup>†</sup>A *unimodular matrix* is a square matrix with integer elements and a determinant of  $\pm 1$ .

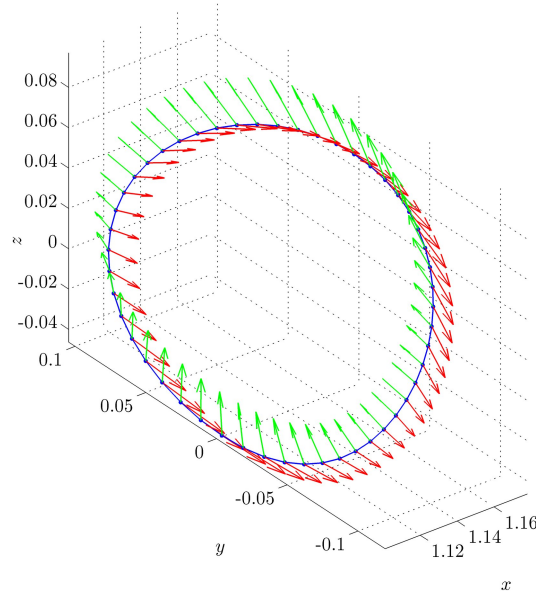


**Figure 2. Eigenvector components  $\text{Re}[\mathbf{y}(\theta_1)]$  and  $\text{Im}[\mathbf{y}(\theta_1)]$  around halo orbit.**

eigenvector of  $\Phi_{2\pi}(\theta_1)$  is selected to be

$$\mathbf{y}(\theta_1) := e^{-i\alpha\theta_1/2\pi} \Phi_{\theta_1}(0) \mathbf{y}(0). \quad (12)$$

The state transition matrix  $\Phi_{\theta_1}(0)$  not only shifts the eigenvector  $\mathbf{y}(0)$  to correspond to point  $\bar{\mathbf{u}}(\theta_1)$ , but it also follows the rotation about the periodic orbit from the flow. The term  $e^{-i\alpha\theta_1/2\pi}$  corresponds to a rotation in the complex plane by the angle  $-\alpha\theta_1/2\pi$ , canceling the rotation from the flow. As a consequence, equation (12) is defined such that  $\mathbf{y} : \mathbb{T}^1 \rightarrow \mathbb{C}^n$  is periodic; for example,  $\mathbf{y}(2\pi) = e^{-i\alpha} \Phi_{2\pi}(0) \mathbf{y}(0) = e^{-i\alpha} e^{i\alpha} \mathbf{y}(0) = \mathbf{y}(0)$ .

Now define a torus function perturbation  $\hat{\mathbf{u}} : \mathbb{T}^2 \rightarrow \mathbb{R}^n$ ,

$$\begin{aligned} \hat{\mathbf{u}}(\theta_1, \theta_2) &:= \text{Re} \left[ e^{i\theta_2} \mathbf{y}(\theta_1) \right] \\ &= \cos \theta_2 \text{Re} [\mathbf{y}(\theta_1)] - \sin \theta_2 \text{Im} [\mathbf{y}(\theta_1)]. \end{aligned} \quad (13)$$

Note that for each  $\theta_1$ ,  $\hat{\mathbf{u}}(\theta_1, \cdot)$  is an ellipse in  $\mathbb{R}^n$  with axes  $\text{Re}[\mathbf{y}(\theta_1)]$  and  $\text{Im}[\mathbf{y}(\theta_1)]$ . For example, the evolution of the axes for a halo orbit in the CR3BP appears in Figure 2. From the definition in equation (13), it can be demonstrated that the monodromy matrix  $\Phi_{2\pi}(\theta_1)$  maps a point  $\hat{\mathbf{u}}(\theta_1, \theta_2)$  on this ellipse to a point  $\hat{\mathbf{u}}(\theta_1, \theta_2 + \alpha)$  shifted by angle  $\alpha$  on the same ellipse:

$$\begin{aligned} \Phi_{2\pi}(\theta_1) \hat{\mathbf{u}}(\theta_1, \theta_2) &= \Phi_{2\pi}(\theta_1) \text{Re} \left[ e^{i\theta_2} \mathbf{y}(\theta_1) \right] \\ &= \text{Re} \left[ e^{i\theta_2} \Phi_{2\pi}(\theta_1) \mathbf{y}(\theta_1) \right] \\ &= \text{Re} \left[ e^{i\theta_2} e^{i\alpha} \mathbf{y}(\theta_1) \right] \\ &= \hat{\mathbf{u}}(\theta_1, \theta_2 + \alpha). \end{aligned} \quad (14)$$

Therefore, a linear approximation of the torus is available from

$$\mathbf{u}(\theta_1, \theta_2) = \bar{\mathbf{u}}(\theta_1) + \epsilon \hat{\mathbf{u}}(\theta_1, \theta_2), \quad (15)$$

where  $\epsilon \in \mathbb{R}$  fixes the size of the torus. Its frequencies are  $\boldsymbol{\omega} = (\omega_1, \omega_2) = (2\pi/T_1, \alpha/T_1)$ . Note that any angle  $\alpha = \alpha_0 + 2\pi k$ ,  $k \in \mathbb{Z}$ , such that  $\cos \alpha + i \sin \alpha$  is an eigenvalue of the monodromy matrix, can be selected since a unimodular transformation of the frequency vector  $\boldsymbol{\omega}$  also corresponds to a suitable parameterization of the torus. This approach can be generalized without much difficulty to yield initial approximations for tori of dimension  $p > 2$  from periodic orbits having a monodromy matrix with more than one pair of complex conjugate eigenvalues.

### Discretization Scheme

To compute quasi-periodic tori satisfying the invariance PDE in equation (7) and the phase condition in equation (9), these equations are discretized using a central-difference method. This approach was developed by Schilder et al.,<sup>9</sup> and a general overview is currently presented. The torus function  $\mathbf{u}$  of torus  $T$  is evaluated on an  $N_1 \times \dots \times N_p$  grid of circularly-indexed points,  $\tilde{\mathbb{T}}^p := \{\mathbf{j} = (j_1, \dots, j_p) \mid j_i \in \mathbb{Z}/N_i\mathbb{Z}\}$ . The approximated torus function  $\tilde{\mathbf{u}} : \tilde{\mathbb{T}}^p \rightarrow \mathbb{R}^n$  is defined such that  $\tilde{\mathbf{u}}(\mathbf{j}) := \mathbf{u}(\boldsymbol{\theta})$  where  $\theta_i = j_i h_i$  and  $h_i := 2\pi/N_i$ .

Operations equivalent to those on continuous torus functions are developed for the discrete case. Partial differentiation  $\partial/\partial\theta_i$  of  $\mathbf{u}(\boldsymbol{\theta})$  is approximated on the discrete domain by the operator  $\partial_i$ ,

$$\partial_i \tilde{\mathbf{u}}(\mathbf{j}) := \frac{1}{h_i} \sum_{k=-l}^l c_k \tilde{\mathbf{u}}(\dots, j_i + k, \dots), \quad (16)$$

where  $c_k = -c_{-k}$  are the central-difference coefficients. For the second-order approximation of  $\partial\mathbf{u}/\partial\theta_i$ ,  $l = 1$ :  $c_0 = 0$  and  $c_1 = 1/2$ . For the fourth-order approximation,  $l = 2$ :  $c_0 = 0$ ,  $c_1 = 2/3$ , and  $c_2 = -1/12$ . The inner product between two functions  $\tilde{\mathbf{v}}, \tilde{\mathbf{w}} : \tilde{\mathbb{T}}^p \rightarrow \mathbb{R}^n$  is defined such that

$$\langle \tilde{\mathbf{v}}, \tilde{\mathbf{w}} \rangle := \frac{1}{N_1 \dots N_p} \sum_{\mathbf{j} \in \tilde{\mathbb{T}}^p} \langle \tilde{\mathbf{v}}(\mathbf{j}), \tilde{\mathbf{w}}(\mathbf{j}) \rangle, \quad (17)$$

which is a discrete version of equation (8). Using these definitions, equations (7) and (9) for a  $p$ -dimensional quasi-periodic torus can be discretized as follows,

$$\mathbf{f}(\tilde{\mathbf{u}}(\mathbf{j})) - \sum_{i=1}^p \omega_i \partial_i \tilde{\mathbf{u}}(\mathbf{j}) = \mathbf{0}, \quad \text{for all } \mathbf{j} \in \tilde{\mathbb{T}}^p, \quad (18)$$

$$\langle \partial_i \tilde{\mathbf{u}}_0, \tilde{\mathbf{u}} \rangle = 0, \quad \text{for all } i \in \{1, \dots, p\}, \quad (19)$$

where  $\tilde{\mathbf{u}}_0$  is the discrete torus function of a nearby family member  $T_0$  that is already computed.

### Continuation of Families

For this application, consider computing quasi-periodic tori that lie in two-parameter families, particularly  $p = 2$ -dimensional tori in the CR3BP. While schemes exist for multiple-parameter continuation, most are designed for one-parameter families. To reduce the family to a single parameter, a straightforward option is to isolate family members that exist at a specific value of an integral of motion. For the CR3BP the Jacobi constant,  $C$ , from equation (3) is fixed at a certain value  $C_0$  for each of the tori in a family,

$$C(\mathbf{u}) = C_0. \quad (20)$$



Since a quasi-periodic torus can be viewed as the closure of a single orbit, an integral of motion such as the energy-like Jacobi constant is a function of the torus itself and independent of a particular point on the torus.

Once the family is reduced to a single parameter, pseudo-arclength continuation is used to determine a torus  $T$ , corresponding to solution  $(\mathbf{u}, \boldsymbol{\omega}, \boldsymbol{\lambda})$ , a distance  $\Delta s$  from a known torus  $T_0$ . The distance is defined by a single scalar equation that projects the change between the tori down upon the family tangent at  $T_0$ ,

$$\langle \mathbf{u} - \mathbf{u}_0, \mathbf{u}'_0 \rangle + \langle \boldsymbol{\omega} - \boldsymbol{\omega}_0, \boldsymbol{\omega}'_0 \rangle + \langle \boldsymbol{\lambda} - \boldsymbol{\lambda}_0, \boldsymbol{\lambda}'_0 \rangle = \Delta s. \quad (21)$$

The tangent direction  $(\mathbf{u}'_0, \boldsymbol{\omega}'_0, \boldsymbol{\lambda}'_0)$  is normalized such that  $\|\mathbf{u}'_0\|^2 + \|\boldsymbol{\omega}'_0\|^2 + \|\boldsymbol{\lambda}'_0\|^2 = 1$ . If  $T_{-1}$  and  $T_0$  are two previous solutions, the direction of the family tangent can be approximated by normalizing  $(\mathbf{u}_0 - \mathbf{u}_{-1}, \boldsymbol{\omega}_0 - \boldsymbol{\omega}_{-1}, \boldsymbol{\lambda}_0 - \boldsymbol{\lambda}_{-1})$ .

The invariance PDE from equation (7), phase condition in equation (9), Jacobi constant constraint specified in equation (20), and pseudo-arclength equation (21) produce a unique quasi-periodic torus as a solution. The equations can be written in discretized form for tori of dimension  $p = 2$  in the CR3BP and are summarized in the following system of equations:

$$\mathbf{0} = \mathbf{F}_{1j}(\tilde{\mathbf{u}}, \boldsymbol{\omega}) := \mathbf{f}(\tilde{\mathbf{u}}(j)) - \sum_{i=1}^2 \omega_i \partial_i \tilde{\mathbf{u}}(j), \quad \text{for all } j \in \tilde{\mathbb{T}}^2; \quad (22a)$$

$$0 = F_{2i}(\tilde{\mathbf{u}}) := \langle \partial_i \tilde{\mathbf{u}}_0, \tilde{\mathbf{u}} \rangle, \quad \text{for all } i \in \{1, 2\}; \quad (22b)$$

$$0 = F_3(\tilde{\mathbf{u}}) := \frac{1}{N_1 N_2} \sum_{j \in \tilde{\mathbb{T}}^2} C(\tilde{\mathbf{u}}(j)) - C_0; \quad (22c)$$

$$0 = F_4(\tilde{\mathbf{u}}, \boldsymbol{\omega}) := k_u \langle \tilde{\mathbf{u}} - \tilde{\mathbf{u}}_0, \tilde{\mathbf{u}}'_0 \rangle + k_\omega \langle \boldsymbol{\omega} - \boldsymbol{\omega}_0, \boldsymbol{\omega}'_0 \rangle - \Delta s. \quad (22d)$$

The Jacobi constant  $C$  is averaged over the entire torus in equation (22c) to distribute numerical sensitivities. Also, coefficients  $k_u$  and  $k_\omega$  are added to the pseudo-arclength equation (22d) to allow more control over the stepping process. Typical choices are  $k_u = 1$  and  $k_\omega = 0$  to prevent falling back to a periodic orbit where  $\tilde{\mathbf{u}} - \tilde{\mathbf{u}}_0 = \mathbf{0}$  but  $\boldsymbol{\omega} - \boldsymbol{\omega}_0 \neq \mathbf{0}$ . There is no  $\langle \boldsymbol{\lambda} - \boldsymbol{\lambda}_0, \boldsymbol{\lambda}'_0 \rangle$  term since the CR3BP model does not have any external parameters.

The system of equations (22) is solved for  $\tilde{\mathbf{u}}$  and  $\boldsymbol{\omega}$  using a Newton method. If  $\tilde{\mathbf{u}}$  is represented as a column vector of length  $nN_1N_2$ , the system of equations to be solved is

$$\left[ \begin{array}{cc} \partial \mathbf{F}_1 / \partial \tilde{\mathbf{u}} & \partial \mathbf{F}_1 / \partial \boldsymbol{\omega} \\ \partial \mathbf{F}_2 / \partial \tilde{\mathbf{u}} & \mathbf{0} \\ \partial F_3 / \partial \tilde{\mathbf{u}} & \mathbf{0} \\ \partial F_4 / \partial \tilde{\mathbf{u}} & \partial F_4 / \partial \boldsymbol{\omega} \end{array} \right] \bigg|_{\tilde{\mathbf{u}}, \boldsymbol{\omega}} \begin{pmatrix} \delta \tilde{\mathbf{u}} \\ \delta \boldsymbol{\omega} \end{pmatrix} = - \begin{pmatrix} \mathbf{F}_1(\tilde{\mathbf{u}}, \boldsymbol{\omega}) \\ \mathbf{F}_2(\tilde{\mathbf{u}}) \\ F_3(\tilde{\mathbf{u}}) \\ F_4(\tilde{\mathbf{u}}, \boldsymbol{\omega}) \end{pmatrix}, \quad (23)$$

where  $\tilde{\mathbf{u}} \mapsto \tilde{\mathbf{u}} + \delta \tilde{\mathbf{u}}$  and  $\boldsymbol{\omega} \mapsto \boldsymbol{\omega} + \delta \boldsymbol{\omega}$  are updated at each iteration. Details of the sparse structure of submatrix  $\partial \mathbf{F}_1 / \partial \tilde{\mathbf{u}}$  in the Jacobian is available in Schilder et al.<sup>9</sup> Note that the structure of the CR3BP leads to an  $(nN_1N_2+4) \times (nN_1N_2+2)$  Jacobian matrix. Though this linear system appears to be overdetermined, KAM theory suggests that for a Hamiltonian system such as the CR3BP, a solution does, in fact, exist. Therefore, two columns can be added to make the Jacobian square, provided they are not already in the column space.

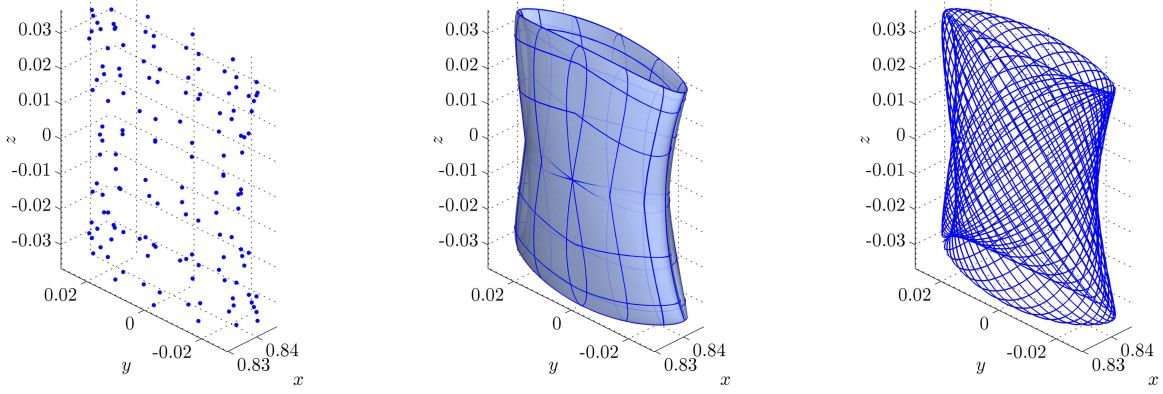


**Figure 3.** Mesh points, invariant torus surface, and quasi-periodic trajectory corresponding to Lissajous orbit.

Consider these columns as corresponding to two “artificial” external parameters  $\lambda_1 = \lambda_2 = 0$  that do not affect the dynamics at value zero. A suitable choice is to randomly generate vectors  $\mathbf{v}_1, \mathbf{v}_2 \in \mathbb{R}^{nN_1N_2+4}$  resulting in the linear system

$$\left[ \begin{array}{cc} \partial \mathbf{F}_1 / \partial \tilde{\mathbf{u}} & \partial \mathbf{F}_1 / \partial \boldsymbol{\omega} \\ \partial \mathbf{F}_2 / \partial \tilde{\mathbf{u}} & \mathbf{0} \\ \partial \mathbf{F}_3 / \partial \tilde{\mathbf{u}} & \mathbf{0} \\ \partial \mathbf{F}_4 / \partial \tilde{\mathbf{u}} & \partial \mathbf{F}_4 / \partial \boldsymbol{\omega} \end{array} \middle| \begin{array}{cc} \mathbf{v}_1 & \mathbf{v}_2 \end{array} \right] \bigg|_{\tilde{\mathbf{u}}, \boldsymbol{\omega}} \begin{pmatrix} \delta \tilde{\mathbf{u}} \\ \delta \boldsymbol{\omega} \\ \delta \lambda_1 \\ \delta \lambda_2 \end{pmatrix} = - \begin{pmatrix} \mathbf{F}_1(\tilde{\mathbf{u}}, \boldsymbol{\omega}) \\ \mathbf{F}_2(\tilde{\mathbf{u}}) \\ \mathbf{F}_3(\tilde{\mathbf{u}}) \\ \mathbf{F}_4(\tilde{\mathbf{u}}, \boldsymbol{\omega}) \end{pmatrix}. \quad (24)$$

Since  $\mathbf{v}_1$  and  $\mathbf{v}_2$  are random, the Jacobian should be square and nonsingular. A standard sparse linear solver can be used to compute update  $(\delta \tilde{\mathbf{u}}, \delta \boldsymbol{\omega}, \delta \lambda_1, \delta \lambda_2)$  where  $\delta \lambda_1, \delta \lambda_2 \approx 0$ .

### Generating Orbit on Torus

Since the torus function  $\mathbf{u}$  possesses a natural parameterization via angles  $\boldsymbol{\theta} \in \mathbb{T}^p$ , it is well-suited to generating individual orbits. A single quasi-periodic orbit can be determined on a torus by interpolating the discretized torus function  $\tilde{\mathbf{u}}$  on the evenly-spaced mesh points  $\tilde{\mathbb{T}}^p$ . In the current study, a  $p = 2$ -parameter cubic spline  $\tilde{\mathbf{u}}^* : \mathbb{T}^2 \rightarrow \mathbb{R}^n$  is generated over the domain  $[0, 2\pi] \times [0, 2\pi]$  with periodic end conditions. This is possible using a variety of software packages. Then, from any starting point  $\boldsymbol{\theta}_0 \in \mathbb{T}^2$ , the state at time  $t$  is approximated as

$$\mathbf{x}(t) = \tilde{\mathbf{u}}^*((\boldsymbol{\theta}_0 + \boldsymbol{\omega}t) \pmod{2\pi}). \quad (25)$$

A trajectory generated in this manner is suitable for input to a higher-order corrections scheme or to initiate the transition to an ephemeris model using a process such as multiple shooting. Since the cubic spline can be evaluated efficiently once it is computed, quasi-periodic orbits from various starting points  $\boldsymbol{\theta}_0$  can be generated with minimal computational effort.

Examples of this scheme applied to a Lissajous trajectory and a quasi-halo orbit are presented in Figures 3 and 4, which illustrate the mesh points from the discretization of the PDE, the corresponding invariant torus surface generated from a two-parameter cubic spline, and the quasi-periodic orbit that lies on the torus surface.

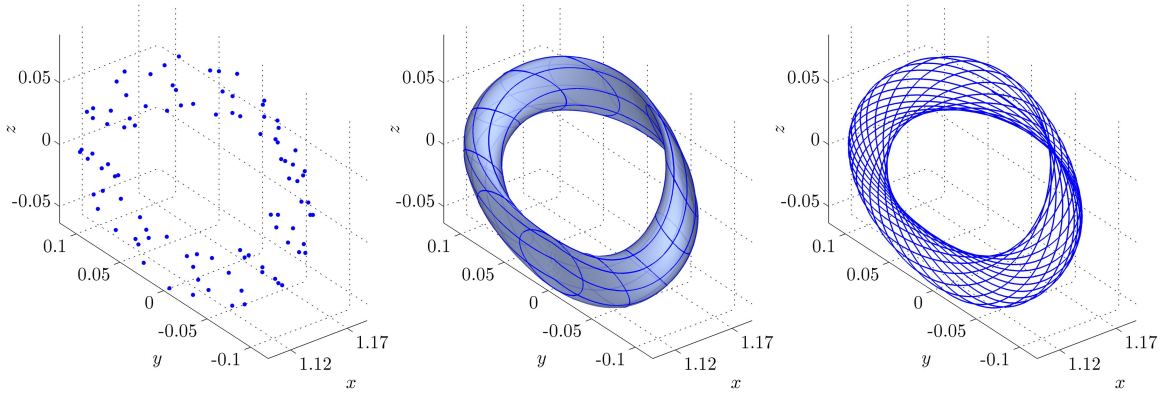


**Figure 4.** Mesh points, invariant torus surface, and quasi-periodic trajectory corresponding to quasi-halo orbit.

## RESULTS

The current approach is the basis of a preliminary framework for computing quasi-periodic tori in the CR3BP. Some sample results are presented in the Earth-Moon system ( $\mu = 0.01215$ ) to test the methodology, but this is not intended to be a complete study. The computation scheme is implemented in MATLAB<sup>®</sup> R2009b on a laptop with a 2.66 GHz Intel<sup>®</sup> Core<sup>™</sup> 2 Duo processor. Each Newton update of equation (24) is solved using the sparse LU factorization built into MATLAB, and the Spline Toolbox is used to generate the quasi-periodic trajectory from equation (25).

A quasi-periodic torus about an  $L_1$  Lyapunov orbit with Jacobi constant  $C = 3.179$  is approximated using equation (15). This choice of Jacobi constant is not unique, and any  $L_1$  Lyapunov orbit with center component can be selected. The torus is computed on an  $N_1 \times N_2 = 40 \times 40$  grid with fourth-order central differencing. Pseudo-arclength continuation is then used to generate a family of tori with a fixed value  $C$ . Six members of this family, known as Lissajous tori, appear in Figure 5. These Lissajous orbits terminate at an  $L_1$  vertical orbit, also with  $C = 3.179$ . A total of 13 members of the family are computed in 90 seconds with roughly 95 percent of the time spent solving the linear system from equation (24). The Jacobian is of dimension  $9,604 \times 9,604$  with roughly 0.17 percent of the elements nonzero. Similar quasi-periodic families are observed to connect the planar Lyapunov periodic orbits about  $L_2$  and  $L_3$  and the short-period orbits about  $L_4$  and  $L_5$  to the corresponding vertical periodic orbits.

The halo family of periodic orbits branches from the planar Lyapunov orbits about the collinear libration points. Many halo orbits have a center component. An example family of  $L_2$  quasi-halo tori with Jacobi constant  $C = 3.132$  is plotted in Figure 6. Each torus is computed on an  $N_1 \times N_2 = 75 \times 25$  grid, which corresponds to an  $11,254 \times 11,254$  Jacobian that is about 0.15 percent dense. It requires 58 seconds total to compute 10 family members. The continuation runs into difficulty when the “edges” of the tori get close to the  $xy$ -plane; for example, see the torus in the bottom, right of Figure 6. In addition, since the tori are computed on a uniform mesh, there are numerical difficulties generating a family from a halo that passes near to a primary body where the dynamics change much faster.

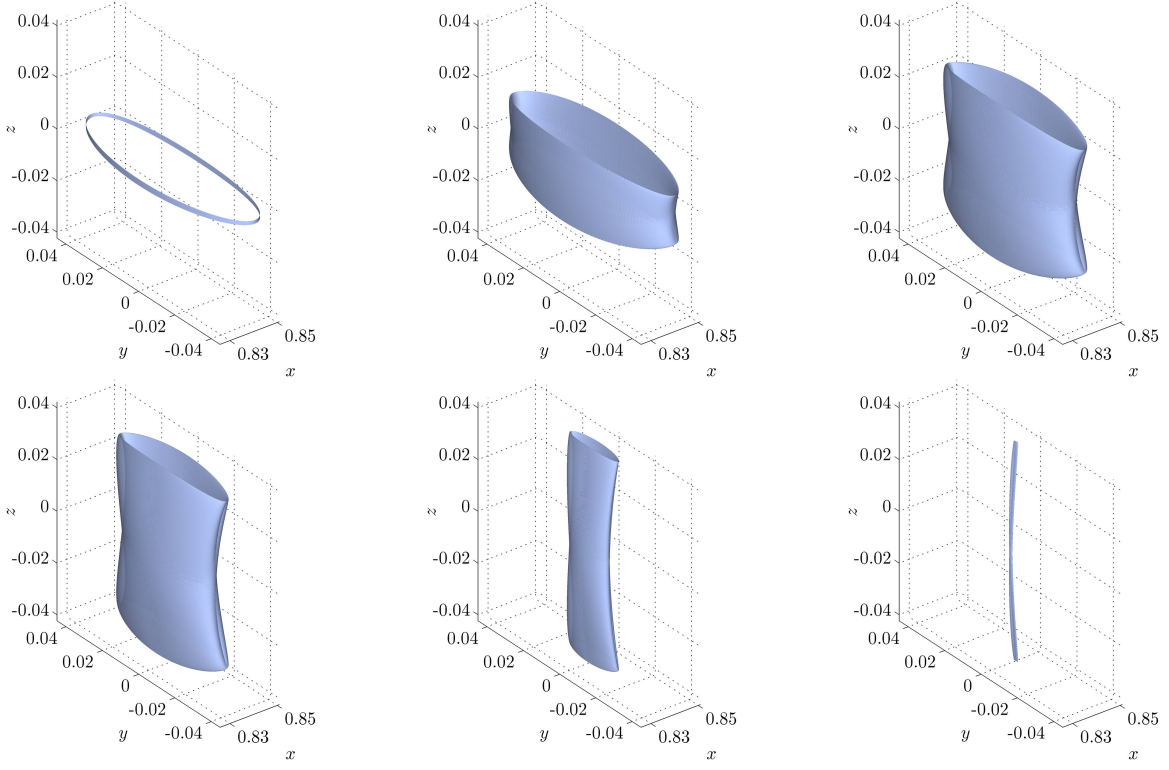


Figure 5. Family of Earth-Moon  $L_1$  Lissajous tori ( $C = 3.179$ ).

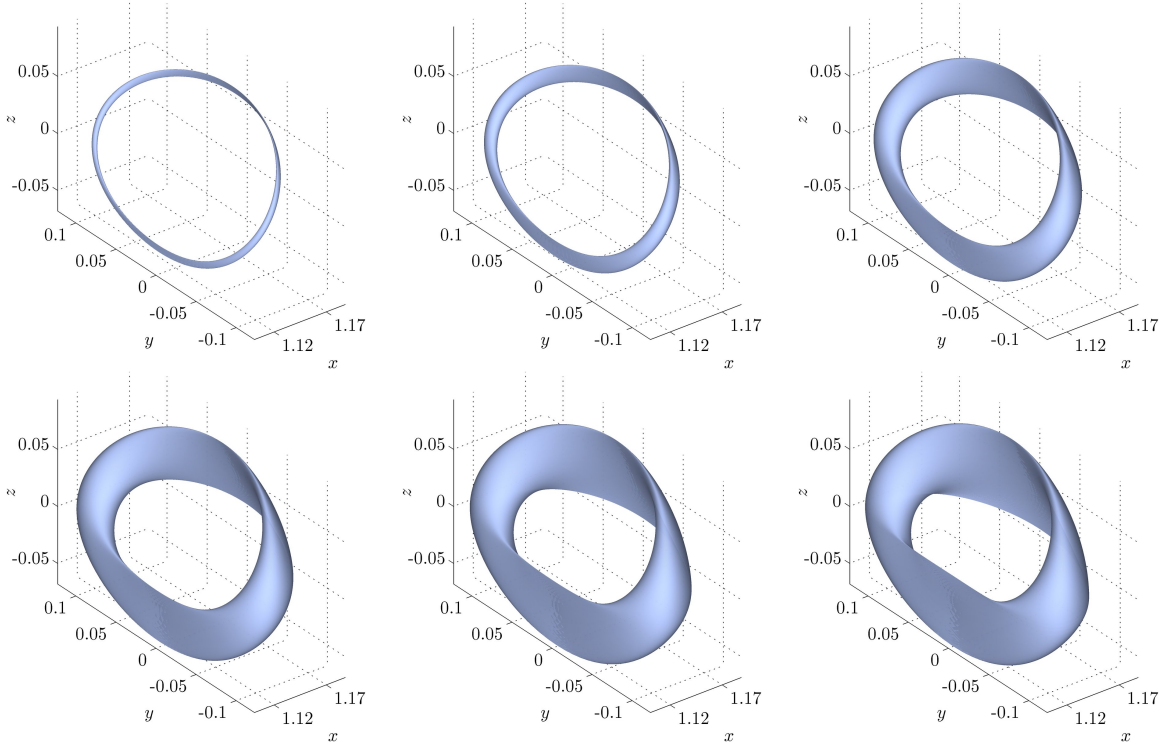
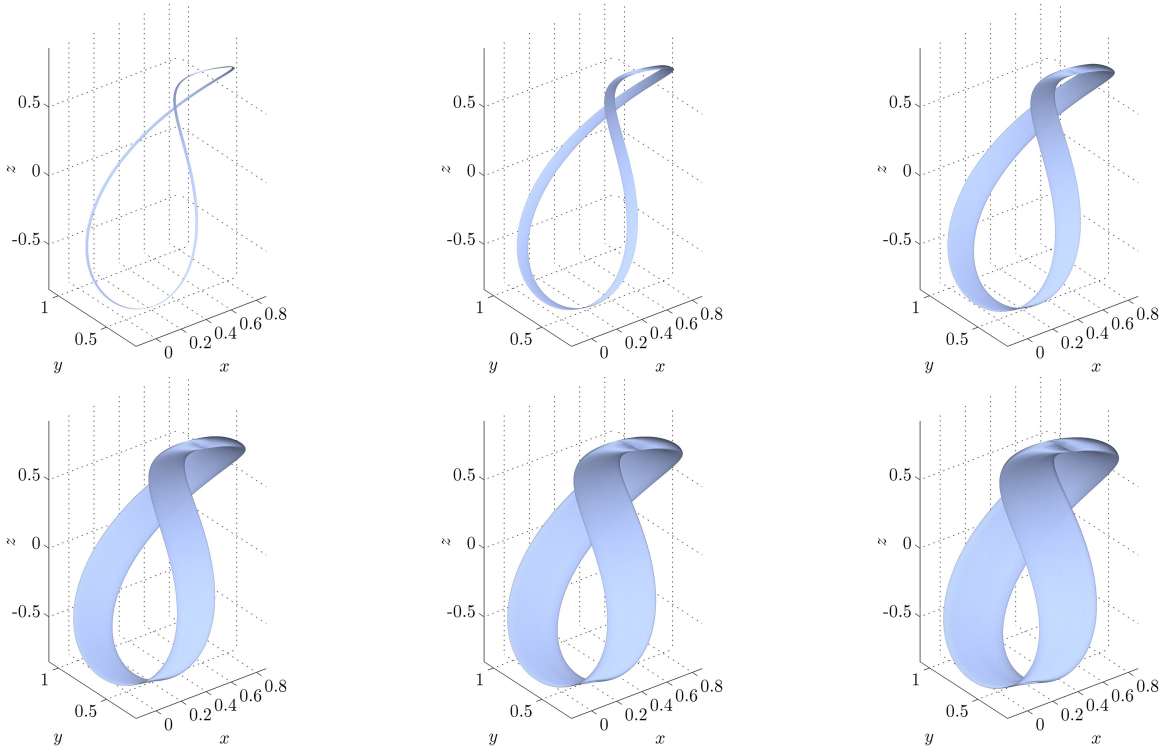


Figure 6. Family of Earth-Moon  $L_2$  quasi-halo tori ( $C = 3.132$ ).



**Figure 7. Family of quasi-periodic tori ( $C = 2.012$ ) about Earth-Moon  $L_4$  point.**

The computation scheme only requires an appropriate initial guess for a torus, and does not require any modification between families. A family of periodic orbits bifurcates from the vertical orbits about the triangular libration points  $L_4$  and  $L_5$ . This family of orbits, labeled the  $W$  family in Doedel et al.,<sup>10</sup> includes a center component. Even though the orbits do not possess any symmetries and there is no prior insight into the appearance of a quasi-periodic torus about this orbit, the algorithm is still successful. The family of tori about a  $W$  periodic orbit with Jacobi constant  $C = 2.012$  appears in Figure 7. Part of a quasi-periodic trajectory on the surface of one of the tori is plotted in Figure 8.

## CONCLUSION

This paper introduces a method for computing quasi-periodic invariant tori in the CR3BP. The approach is based on a scheme developed for generic dynamical systems, and suitable modifications are incorporated for the CR3BP's special structure. An invariance PDE and phase condition produce a natural parameterization of the torus function, which can be initialized from a periodic orbit with a center component. Pseudo-arclength continuation is then used to generate families of two-dimensional tori with a fixed Jacobi constant. The discretized system is numerically implemented and used to compute sample families of quasi-periodic tori in the vicinity of the Earth-Moon CR3BP libration points. A quasi-periodic orbit lying on the torus can easily be computed using a spline interpolation.

Future work includes error analysis of the quasi-periodic tori that are generated and a mesh refinement scheme to enable computation of tori near the primaries. Exploiting high-

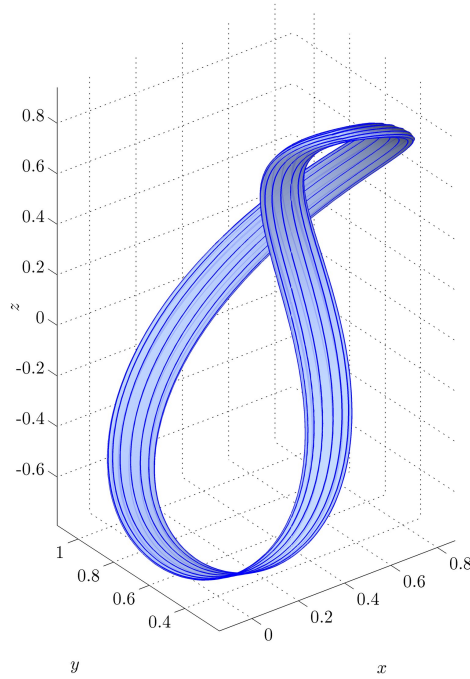


**Figure 8. Quasi-periodic torus and orbit about Earth-Moon  $L_4$  point.**

performance computing tools also might allow finer meshes to be evaluated. In addition, a stability analysis of the quasi-periodic orbits is warranted for the mission design applications.

## ACKNOWLEDGMENTS

This work was conducted at Purdue University with support from the School of Aeronautics and Astronautics and the National Science Foundation (NSF) Graduate Research Fellowship Program.

## REFERENCES

- [1] G. Gómez, À. Jorba, J. J. Masdemont, and C. Simó, “Study of the Transfer from the Earth to a Halo Orbit Around the Equilibrium Point  $L_1$ ,” *Celestial Mechanics and Dynamical Astronomy*, Vol. 56, No. 4, 1993, pp. 541–562.
- [2] K. C. Howell, B. T. Barden, and M. W. Lo, “Application of Dynamical Systems Theory to Trajectory Design for a Libration Point Mission,” *Journal of the Astronautical Sciences*, Vol. 45, No. 2, 1997, pp. 161–178.
- [3] B. T. Barden and K. C. Howell, “Fundamental Motions Near Collinear Libration Points and Their Transitions,” *Journal of the Astronautical Sciences*, Vol. 46, No. 4, 1998, pp. 361–378.
- [4] À. Jorba and J. J. Masdemont, “Dynamics in the Center Manifold of the Restricted Three-Body Problem,” *Physica D*, Vol. 132, No. 1–2, 1999, pp. 189–213.
- [5] G. Gómez, J. J. Masdemont, and C. Simó, “Quasihalo Orbits Associated with Libration Points,” *Journal of the Astronautical Sciences*, Vol. 46, No. 2, 1998, pp. 135–176.
- [6] À. Jorba, “Numerical Computation of the Normal Behavior of Invariant Curves of  $n$ -Dimensional Maps,” *Nonlinearity*, Vol. 14, No. 5, 2001, pp. 943–976.
- [7] À. Jorba and E. Olmedo, “On the Computation of Reducible Invariant Tori in a Parallel Computer,” Preprint, 2008.

- [8] G. Gómez and J. M. Mondelo, “The Dynamics Around the Collinear Equilibrium Points of the RTBP,” *Physica D*, Vol. 157, No. 4, 2001, pp. 283–321.
- [9] F. Schilder, H. M. Osinga, and W. Vogt, “Continuation of Quasi-Periodic Invariant Tori,” *SIAM Journal on Applied Dynamical Systems*, Vol. 4, No. 3, 2005, pp. 459–488.
- [10] E. J. Doedel, V. A. Romanov, R. C. Paffenroth, H. B. Keller, D. J. Dichmann, J. Galán-Vioque, and A. Vanderbauwhede, “Elemental Periodic Orbits Associated with the Libration Points in the Circular Restricted 3-Body Problem,” *International Journal of Bifurcation and Chaos*, Vol. 17, No. 8, 2007, pp. 2625–2677.
- [11] H. W. Broer, G. B. Huitema, and M. B. Sevryuk, *Quasi-Periodic Motions in Families of Dynamical Systems*, Berlin: Springer-Verlag, 1996.